DALTON
FULL PAPER

# *N*,*N*′-Di(tolyl)formamidinate complexes of potassium: studies of ancillary donor imposed molecular and supramolecular structure

**Jens Baldamus,†[a] Christiane Berghof,†[a] Marcus L. Cole,[a] David J. Evans,[a] Evamarie Hey-Hawkins[b] and Peter C. Junk*[a]**

[a] *School of Chemistry, Monash University, P.O. Box 23, Clayton, Vic 3800, Australia. E-mail: peter.junk@sci.monash.edu.au*
[b] *Institut für Anorganische Chemie, Universität Leipzig, Johannisallee 29, D-04103 Leipzig, Germany*

***Received 26th June 2002, Accepted 29th August 2002***
***First published as an Advance Article on the web 15th October 2002***

Treatment of *N*,*N*′-di(tolyl)formamidines ((Tol)NC(H)N(H)(Tol)) HFTolP (TolP = *para*-tolyl) and HFTolM (TolM = *meta*-tolyl) with potassium hydride affords the colourless crystalline formamidinate complexes $[\{K_2(FTolP)_2(THF)_3\}_\infty]$, **1**, and $[\{(K_2(FTolM)_2(THF)_3)\cdot THF\}_\infty]$, **2** when conducted in THF. An analogous HFTolP preparation in 1,2-dimethoxyethane yields the DME analogue of **1**; $[\{K(FTolP)(DME)\}_\infty]$, **3**, whilst treatment of HFTolP with potassium hydride in toluene followed by stoichiometric addition of 18-crown-6 gives monomeric [K(FTolP)(18-crown-6)], **4**. Compounds **1**–**4** have been characterised by spectroscopy ($^1$H NMR, $^{13}$C NMR and FTIR) and single crystal XRD. In the solid-state **1**–**3** display one-dimensional polymeric structures that exhibit $\mu$-$\eta^2$:$\eta^2$-coordinated formamidinates. These approach $\eta^3$-diazaallyl contact by virtue of dinuclear bridging. Compound **4**, the first example of a poly-ether crown adducted monomeric Group 1 amidinate, exhibits both inter- and intra-molecular C–H ⋯ O hydrogen bonding in the solid-state. Supramolecularly, this renders **4** a two-dimensional hydrogen-bonded polymer. Complexes **1**–**4** are discussed with respect to known potassium benzamidinate/guanidinate complexes and related amido-2-pyridyl ligand species.

## Introduction

The synthetic utility of alkali metal amide derivatives and the acknowledged relationship of structure to reactivity has encouraged the widespread crystallographic study of *N*-centred Group 1 organometallic species.[1] To date, these studies have identified several trends which result from amide steric bulk and metal electropositivity.[2–8] Lamentably, whilst the chemistry of lithium amides has been comprehensively investigated the structural study of heavier Group 1 complexes has remained scarce.[1] This is presumably because there is little advantage in handling these more reactive reagents as Brönsted bases or nucleophiles.[9–13] Nevertheless, given that heavier Group 1 metal–nitrogen bonds exhibit higher polarity than lithium counterparts, and their considerable increase in ionic radius,[14] the inclusion of ancillary donors in heavier Group 1 species, *e.g.* potassium amides, should be more pronounced. Accordingly, significant structural diversity may result from minor modification of the reaction medium.

Historically, Group 1 metallated *N*,*N*′-di(aryl)formamidines have been perceived as precursors to close-contact bimetallic 'lantern-type' transition metal complexes,[15–18] *e.g.* $[V_2(FTolP)_4]$[19] (FTolP = *N*,*N*′-di(*para*-tolyl)formamidinate, (*para*-$CH_3C_6H_4$)NC(H)N(*para*-$CH_3C_6H_4$)), and have thus evaded structural characterisation due to supposed low-novelty. In-view of the current surfeit of p-block metal amidinate species[20–26] invited by the prolific catalysis studies of Jordan *et al.*[27–29] we have chosen to address the lack of such study. Prior to our involvement in this field there existed just one report describing the structural authentication of Group 1 and 2 formamidinates.[30] This contained both $[\{Li(\mu\text{-}\eta^1\text{:}\eta^2\text{-}FTolP)(Et_2O)\}_2]$ and $[(\mu\text{-}Cl)_2(\mu\text{-}THF)\{Mg(\eta^2\text{-}FPh)(THF)_2\}_2]$ (FPh = *N*,*N*′-di(phenyl)formamidinate, PhNC(H)NPh), and suggested that the facility by which Group 1 formamidinates lose donor solvent was culpable for their archival absence. Our on-going study into *s*-block formamidinate complexes has afforded several lithium, sodium and magnesium species, *viz.* $[Li(DME)_3][Li_2(\mu\text{-}\eta^1\text{:}\eta^1\text{-}FTolP)_3]$,[31] $[\{Na(\mu\text{-}\eta^2\text{:}\eta^1\text{-}FTolP)(\mu\text{-}\eta^1\text{:}\eta^1\text{-}DME)\}_2]$[31] and $[Mg(\eta^2\text{-}FTolP)_2(THF)_2]$,[32] that display diverse formamidinate binding modes indicative of the flexible geometric and steric constraints of formamidinates relative to the encumbered alkyl/aryl/amido substituted backbone of amidinates/guanidinates. Given these preliminary studies, the structural chemistry of s-block formamidinates could be more bountiful than previously anticipated.

The adverse inclusion of alkali-metal halides in lanthanoid complexes prepared by metathesis is often frustrated by the precipitation of insoluble heavy Group 1 halide salts from ethereal reaction media.[33,34] Our desire to prepare f-block complexes of the formamidinates, which have no precedent, *via* metathetical exchange has prompted us to investigate the potassium chemistry of both high and low steric bulk *N*,*N*′-di(aryl)-formamidinates. Thus far, this has produced the novel FMes/HFMes (FMes = *N*,*N*′-di(mesityl)formamidinate, (2,4,6-$Me_3C_6H_2$)NC(H)N(2,4,6-$Me_3C_6H_2$)) complex $[K\{(\eta^6\text{-Mes})NC(H)N(Mes)\}\{(\eta^6\text{-Mes})NC(H)NH(Mes)]$, **5**,[35] which displays a bound HFMes ligand with suppressed reactivity resulting from sterically hindered mesityl groups (Mes/mesityl = 2,4,6-trimethylphenyl). The resilience of **5** to both HFMes/Lewis base solvent exchange and reaction with excess potassium reagent invites that similar studies be undertaken with formamidines of lesser steric bulk and lower potential aromatic electron density, *e.g.* HFTolP, in-order to prepare reagents suitable for metathesis. To date, aside from **5**, the structures of just three monoanionic benzamidinate/guanidinate complexes of potassium have been reported.[36–38] Without exception these exhibit di-potassium di-amidinate subunits that display symmetrical

† On leave from the Institut für Anorganische Chemie, Universität Leipzig, Johannisallee 29, D-04103 Leipzig, Germany.

μ-η²:η²-diazaallyl bonding with NCN carbon–potassium contacts approaching η³-diazaallyl ligation (mean NCN plane to NKN plane angle 39.34°).[36–38] To supplement these examples there are two anionic β-dinitrogen ligand complexes of potassium based upon the amido-2-pyridyl frame (also NCN anionic donors) that also illustrate μ-η²:η²-bound dinuclear motifs.[39,40] Unlike the benzamidinate/guanidinate species mentioned, these contain ancillary/solvent donors that promote low aggregation (*cf.* one benzamidinate species from Lappert *et al.*[37] contains nitrile donors which result from the addition of excess nitrile reagent during preparation and not solvation from the reaction medium). Herein we report the stoichiometric treatment of two sterically 'slight' *N*,*N*′-di(tolyl)formamidines; HFTolP and HFTolM (tolyl = *meta*-tolyl), with potassium hydride under disparate solvent conditions. In all instances solvent or supplementary donors are included in the resulting complexes. In the case of THF or DME (1,2-dimethoxyethane) this encourages rather than limits aggregation. The crystallographic outcomes of this study are discussed with respect to the aforementioned benzamidinate, guanidinate and amido-2-pyridyl ligand complexes.[36–40]

## Results and discussion

Treatment of tetrahydrofuran solutions of HFTolP or HFTolM with a slurry of potassium hydride, also in THF, results in clean deprotonation of the formamidine amino group (Scheme 1).

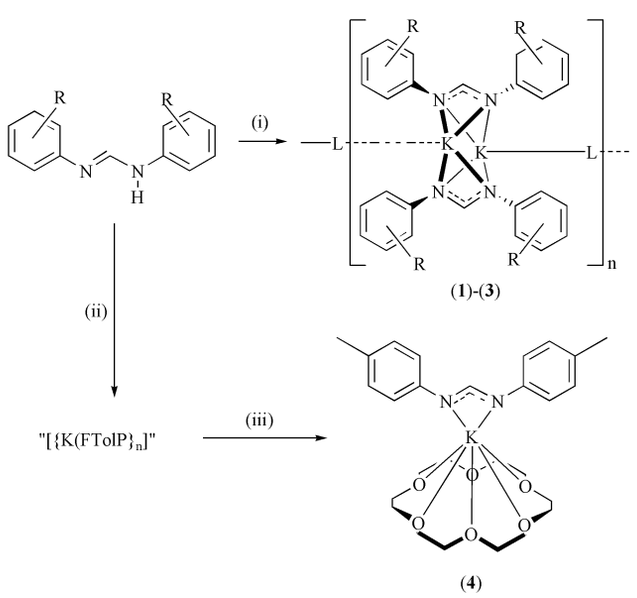


**Scheme 1** Reagents and conditions: (i) 1.0 eq. KH, −1.0 $H_2$ (g), **1**; THF, R = *para*-$CH_3$, L = (μ-THF)$_3$, **2**; THF, R = *meta*-$CH_3$, L = (μ-THF)$_3$, **3**; DME, R = *para*-$CH_3$, L = (μ-η²:η¹-DME)$_2$. (ii) 1.0 eq. KH, −1.0 $H_2$ (g), toluene, R = *para*-$CH_3$. (iii) 1.0 eq. 18-crown-6, toluene.

This renders highly air and moisture sensitive crystalline products that characterise as [K(FTolP)(THF)$_{3/2}$] and [K(FTolM)(THF)$_2$] by $^1$H NMR ($C_6D_6$, non-donating solvent used to preclude further solvation). Spectroscopy confirms deprotonation *via* the absence of resonances attributable to the amino protons of HFTolP and HFTolM (12.28 ppm[30] and 12.15 ppm resp.) and the lack of an N–H stretch at *ca.* 3300 cm$^{-1}$in their FTIR spectra (Nujol, HFTolP N–H stretch 3304 cm$^{-1}$,[31] HFTolM 3313 cm$^{-1}$). The shift of broad NC(H)N $^1$H NMR resonances to 8.15 ppm and 8.92 ppm respectively is also indicative of deprotonation, those of the ligands appearing at 8.01 ppm[31] and 7.59 ppm. The contrast in the position of these new signals suggests a differing solution state nature, whilst the NC(H)N $^{13}$C NMR resonances are placed at 162.3 ppm (**1**) and 158.8 ppm (**2**) ($C_6D_6$). These compare well to those of the THF solvated FTolP complexes of lighter Group 1 elements; [(μ-THF){Li(μ-η¹:η¹-FTolP)(THF)}$_2$]·2THF 8.89 ppm, [Na$_3$(μ$_3$-η²:η¹:η¹-FTolP)$_2$ (μ-η²:η²-FTolP)(THF)$_4$] 8.80 ppm (both $C_6D_6$, no $^{13}$C NMR data available due to low solubility),[31] and contrast with those of the unusual η⁶:η¹-deprotonated FMes ligand in **5** (low temperature $d_8$-THF); 9.13 ppm and 182.5 ppm ($^1$H and $^{13}$C NMR resp.).[35] The absence of temperature dependent redistribution of the FTolP ligands in solution, as per the HFMes/FMes ligands of **5**, suggests the formamidinate ligands of [K(FTolP)(THF)$_{3/2}$] and [K(FTolM)(THF)$_2$] do not equilibrate in $d_6$-benzene. In-tandem with their chemically equivalent tolyl resonances, it could be surmised that there are no aryl–potassium contacts in either species. To assess this the X-ray structure determinations of both [K(FTolP)(THF)$_{3/2}$] and [K(FTolM)(THF)$_2$] were undertaken. A summary of X-ray diffraction data for all complexes is displayed in Table 3. Complexes **1** and **2** were prone to rapid solvent loss (decomposition occurs in seconds with loss of crystallinity) and, hence, mounted in highly viscous hydrocarbon oil followed by immediate cooling under a stream of low temperature dinitrogen gas (123 K). POV-RAY[55] illustrations of each complex can be seen in Figs. 1 and 2 (30% thermal ellipsoids), whilst selected bond-lengths and angles are listed in Table 1.

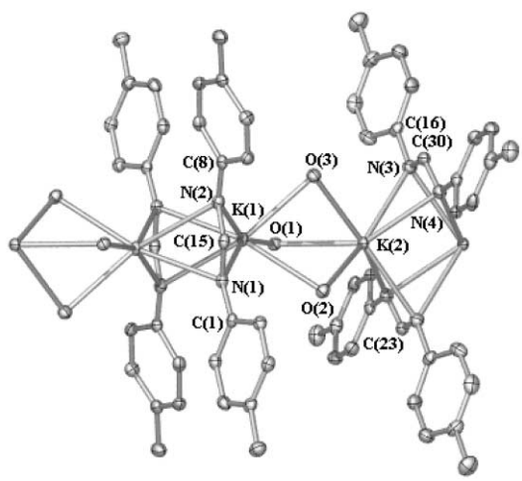


**Fig. 1** Molecular structure of [{K$_2$(μ-η²:η²-FTolP)$_2$(THF)$_3$}$_\infty$], **1**. Two subunits of polymeric structure displayed, hydrogen atoms and tetrahydrofuran $C_4H_8$ tethers omitted for clarity.

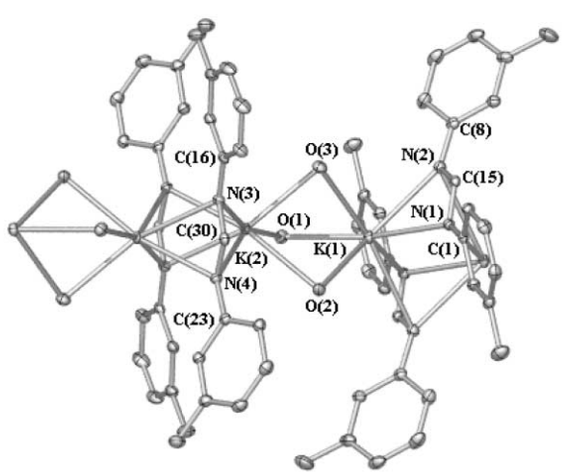


**Fig. 2** Molecular structure of [{K$_2$(μ-η²:η²-FTolM)$_2$(THF)$_3$}$_\infty$], **2**. Two subunits of polymeric structure displayed, hydrogen atoms and tetrahydrofuran $C_4H_8$ tethers omitted for clarity.

Both [{K$_2$(μ-η²:η²-FTolP)$_2$(μ-THF)$_3$}$_\infty$], **1** and [{(K$_2$(μ-η²:η²-FTolM)$_2$(μ-THF)$_3$)·THF}$_\infty$], **2** crystallise in the triclinic space group $P\bar{1}$ with one dinuclear K$_2$(formamidinate)$_2$(THF)$_3$ fragment in the asymmetric unit, and for **2**; one THF molecule of solvation. Their molecular structures consist of discrete

**Table 1** Selected bond-lengths (Å), angles (°) and 'plane to plane' angles (°) for complexes **1**–**4**

| | **1** | **2** | **3** | **4** |
|---|---|---|---|---|
| K(1)–N(1) | 2.933(2) | 2.8223(17) | 3.000(2) | 2.829(2) |
| K(1)–N(2) | 3.017(2) | 3.1385(18) | 2.819(2) | 2.923(2) |
| K(2)–N(3) | 2.843(2) | 2.8566(17) | — | — |
| K(2)–N(4) | 3.148(2) | 2.8617(16) | — | — |
| K(1)#–N(1)[a] | 2.846(3) | 2.7888(16) | 2.987(2) | — |
| K(1)#–N(2)[a] | 2.853(2) | 2.8988(17) | 2.819(2) | — |
| K(2)#–N(3)[a] | 2.864(3) | 2.8005(16) | — | — |
| K(2)#–N(4)[a] | 2.851(2) | 3.1027(19) | — | — |
| C(15)–N(1) | 1.328(3) | 1.322(2) | 1.314(4) | 1.323(3) |
| C(15)–N(2) | 1.328(3) | 1.326(2) | 1.309(4) | 1.323(3) |
| C(30)–N(3) | 1.332(4) | 1.323(2) | — | — |
| C(30)–N(4) | 1.327(4) | 1.323(2) | — | — |
| Mean K–O | 2.82 | 2.82 | 2.81 | 2.93 |
| K(1) ··· K(1)#[a] | 3.4450(12) | 3.5457(19) | 3.4299(13)[b] | — |
| K(1) ··· K(2) | 3.9338(10) | 3.9139(14) | 4.4760(14)[b] | — |
| K(2) ··· K(2)#[a] | 3.4420(12) | 3.4619(13) | — | — |
| | | | | |
| N(1)–C(15)–N(2) | 121.8(2) | 120.66(16) | 121.4(2) | 122.7(3) |
| N(3)–C(30)–N(2) | 121.0(2) | 119.97(16) | — | — |
| N(1)–K(1)–N(2) | 45.87(6) | 45.04(5) | 46.15(7) | 47.59(6) |
| N(3)–K(2)–N(4) | 45.09(7) | 47.22(4) | — | — |
| N(1)–K(1)#–N(2)[a] | 48.04(7) | 47.69(5) | 46.28(7) | — |
| N(3)–K(2)#–N(4)[a] | 47.48(7) | 45.30(4) | — | — |
| Mean NKC : NCN (see Table 2) | 39.90 | 40.97 | 40.08 | 10.4(9) |
| [C(1)–C(6)] : [C(8)–C(13)][c] | 25.68(8) | 52.92(6) | 54.51(7) | 47.98(14) |
| [C(16)–C(21)] : [C(23)–C(28)][c] | 19.73(13) | 32.25(6) | — | — |
| [C(1)–C(6)] : NCN[c] | 26.02(21) | 26.17(17) | 33.12(23) | 14.24(58) |
| [C(8)–C(13)] : NCN[c] | 25.99(17) | 31.80(140 | 23.03(22) | 33.94(41) |
| [C(16)–C(21)] : NCN[c] | 27.08(32) | 8.50(15) | — | — |
| [C(23)–C(28)] : NCN[c] | 28.65(30) | 31.01(9) | — | — |
| $K_2C_2$ : $K_2C_2$[d] | 65.69(8) | 54.86(4) | — | — |

Symmetry transformations used to generate equivalent atoms:[a] For **1** K(1)# $-x, 1-y, -z$, K(2)# $-x, 1-y, 1-z$. For **2** K(1)# $1-x, -y, -z$, K(2)# $1-x, -y, 1-z$. [b] For **3** *intra* $K_2$ formamidinate K(1)# $1-x, -y, 1-z$, *inter*- K(1)# $-x, -y, 1-z$. [c] Carbon atom range denotes tolyl ring phenyl carbons. [d] One potassium and one carbon of each $K_2C_2$ plane generated by symmetry transformations listed in [a] and [b].

$K_2$(formamidinate)$_2$ units linked to two adjacent $K_2$(formamidinate)$_2$ units by six bridging (μ) tetrahydrofuran ligands. Within these units the formamidinate ligands coordinate in a μ-η$^2$:η$^2$-binding mode without supplementary inter-unit contacts. This motif is reminiscent of benzamidinate/guanidinate binding in [{K($C_6H_{11}$NC{N($SiMe_3$)$_2$}N$C_6H_{11}$)}$_2$], **6**,[36] [$K_2${($Me_3$Si)NC(2,5-$Me_2C_6H_3$)NC(2,5-$Me_2C_6H_3$)=C(H)-$SiMe_3$}$_2${(2,5-$Me_2C_6H_3$)CN}$_2$], **7**[37] and [$K_2${($Me_3$Si)NC(Ph)-NC(Ph)=C($SiMe_3$)$_2$}$_2$], **8**,[38] where amidinates bind two potassium metal centres in a near-symmetrical μ-η$^2$:η$^2$-mode. The interrelation of the ligands within **1** and **2** exhibits discrepancies that result courtesy of the tolyl-methyl position. With respect to **1**, in **2** this leads to marginally smaller inter-unit and greater intra-unit potassium–potassium distances (**1**; 3.9338(10) Å and mean 3.443 Å, **2**; 3.9139(14) Å and mean 3.504 Å) due to steric buttressing of the tolyl units with opposing formamidinate aryl groups. This renders the torsion angle between the $K_2C_2$ planes formed by the formamidinate backbone carbons and the potassium atoms 65.69(8)° (**1**) and 54.86(4)° (**2**). Likewise, the mean NCN backbone angles of 121.4° (**1**) and 120.3° (**2**), and the intra-ligand tolyl–tolyl plane torsion angles of 52.92(6)° and 32.25(6)°, suggest greater steric strain within **2** (**1**; 25.68(8)° and 19.73(13)°). The counter-intuitive placement of six out of eight tolyl-methyl groups toward the dinuclear core of **2**, see Fig. 2, presumably exacerbate steric buttressing. Irrespective, this ligand conformation erradicates interaction of the *meta*-methyl groups with the backbone proton of FTolM. Bridging THF interactions are not uncommon in the structural archive,[41] however, to our knowledge the triple-THF-bridged unit of **1** and **2** has no reported precedent.

The generation of a $K_2$(formamidinate)$_2$ unit enforces increased mean NCN plane to NKN plane angles; 39.90° (**1**) and 40.97° (**2**). As-per $K_2$(μ-η$^2$:η$^2$-amidinate)$_2$units within benzamidinate, guanidinate and related anionic β-dinitrogen ligand complexes of potassium (mean NCN plane to NKN planeangles39.34°**6**,39.42°**7**,39.24°**8**,[36–38][$K_2${μ-η$^2$:η$^2$-2-($C_5H_4$N)-NPh}$_2$(tmeda)$_2$] 36.11°[39] and [$K_2${μ-η$^2$:η$^2$-2-($C_5H_4$N)NSi-($CH_3$)$_3$}$_2$(12-crown-4)$_2$] 39.98°)[40] these angles suggest potential potassium–carbon interactions. However, given the mean K ··· $C_{NCN}$ distances of 3.19 Å (**1**) and 3.19 Å (**2**), which are not within the van der Waals/ionic radii approach of potassium and carbon (*ca.* 3.10 Å),[14] it appears the deviation of the KNCN metallocycles from ideal planarity is symptomatic of the dinuclear nature of **1** and **2** rather than a desire for the formamidinate to bind potassium in an η$^3$-diazaallyl mode (mean K–C bond-length within a known K–C bond containing species; [$K_4$(μ-η$^2$:η$^1$-DME)$_2$(μ$_4$-η$^5$:η$^5$:η$^1$:η$^1$-$C_5H_5$)(μ-η$^5$:η$^5$-$C_5H_5$)$_3$]; 3.055 Å).[42] Conversely, as listed in Table 2, this is not borne out by the central placement of NCN backbones such that they interact symmetrically with both flanking potassium atoms. Instead, each potassium experiences significantly greater contact with one formamidinate NCN-carbon relative to its partner ligand. Given the depreciated potassium–carbon bond-lengths this affords (see Table 2), and in-view of the absence of any steric rationale, one can only surmise that the diazaallyl-π-systems of **1** and **2** participate in a degree of donation to the metal of greatest proximity. The placement of the potassium atoms above/below the NCN planes, which is inherent of the bonding motif exhibited by **1** and **2** (and therefore **6**–**8** also), facilitates such donation. In support of this, the structural archive lists mean and median K–C bond lengths of 3.138 Å and 3.091 Å,[43]these are comparable to the shorter K ··· C contacts of both **1** and **2** (see Table 2), which in-turn are below accepted potassium–carbon contacts for aryl-π-donors in benzylic complexes of potassium, *e.g.* [{K(C($SiMe_3$)$_2$$C_6H_5$)}$_\infty$], **9**.[44] Within complex **9** agostic interactions incite potassium–carbon contacts of upto 3.522(2) Å. These supplement recognised η$^2$-aryl potassium–carbon contacts of 3.261(2) Å and 3.351(2) Å. From Table 2, one can see that these are similar to or in excess of those of **1** and **2** thereby bolstering the argument that both

**Table 2** Potassium–carbon distances (Å) and NCN plane to NKN plane angles (°) within the $K_2$formamidinate$_2$ units of complexes **1**–**3**

| | **1**[a] | **2**[b] | **3**[c] |
|---|---|---|---|
| K(1) ··· C(15) | 3.1578(27) | 3.1933(20) | 3.2232(28) |
| K(1) ··· C(15)# | 3.1985(27) | 3.1805(21) | 3.1531(28) |
| K(2) ··· C(30) | 3.3535(28) | 3.1209(19) | — |
| K(2) ··· C(30)# | 3.0666(31) | 3.2819(19) | — |
| N(1)–K(1)–N(2) : N(1)–C(15)–N(2) | 54.73(16) | 52.26(20) | 34.86(25) |
| N(1)–K(1)#–N(2) : N(1)–C(15)–N(2) | 25.52(32) | 30.98(13) | 45.29(27) |
| N(3)–K(2)–N(4) : N(3)–C(30)–N(4) | 28.34(15) | 45.28(10) | — |
| N(3)–K(2)#–N(4) : N(3)–C(30)–N(4) | 50.99(30) | 35.36(12) | — |

Symmetry transformations used to generate equivalent atoms:[a] K(1)#/C(15)# $-x$, $1-y$, $-z$; K(2)#/C(30)# $-x$, $1-y$, $1-z$. [b] K(1)# / C(15)# $1-x$, $-y$, $-z$; K(2)# / C(30)# $1-x$, $-y$, $1-z$. [c] K(1)# / C(15)# $1-x$, $-y$, $1-z$.

structures exhibit near μ-η$^3$:η$^2$- or even μ-η$^3$:η$^3$-formamidinate coordination modes. Meanwhile, the analogous NCN plane to NKN plane angles of compound **6** display less variation than those of **1** and **2** (42.17°, 36.51°, K ··· N 3.085 Å and 3.127 Å,),[36] as does **7** (41.31°, 37.54°, K ··· N 3.159 Å and 3.188 Å),[37] whilst compound **8** exhibits similar deviation (51.30°, 27.19°, K ··· N 3.176 Å and 3.209 Å,).[38] Irrespective, on the basis of the potassium–carbon contacts listed for **9** and the mean/median of potassium–carbon bonds deposited in the Cambridge Crystallographic Structural Database (CCSD)[43,44] these compounds can similarly be considered as the first main group examples of μ-η$^3$:η$^2$- or μ-η$^3$:η$^3$-amidinate binding.[43,45,46] This argument also applies for potassium complexes bearing amido-2-pyridyl ligands (shortest contact within $[K_2\{\mu\text{-}\eta^2\text{:}\eta^2\text{-}2\text{-}(C_5H_4N)NSi(CH_3)_3\}_2(12\text{-crown-}4)_2]$; 3.147 Å), which contain similar anionic NCN donor moieties.[39,40] Most importantly the di-metallic di-amidinate binding motif described by **1**, **2** and **6**–**8** is entirely unique to potassium and has no precedent within transition metal or main group metal amidinate chemistry.

The absence of aryl–potassium interactions within **1** and **2**, as displayed by **5**, can be countenanced by the diminished ability of FTolP and FTolM to participate in aryl-π-donation. We believe that were η$^6$:η$^1$-formamidine/ate ligation to occur during the preparation of **1** and **2**, as occurs with HFMes,[35] the exposed aryl–potassium interaction would easily be overcome by competing THF donation. This would release unmetallated free ligand for subsequent deprotonation. The η$^6$-coordination of mesityl groups is intuitively more robust because of the greater number of appended alkyl groups. These sterically shield and provide greater electron donor capacity to the aryl core.

The bimetallic units of **1** and **2** are reminiscent of the 'lantern-type' transition metal complexes popularised over several decades by, amongst others, Cotton and co-workers.[15–19] However, the lower ratio of ligand to metal in both complexes, which can be greater than one as exemplified by $[Li(DME)_3][Li_2(\mu\text{-}\eta^1\text{:}\eta^1\text{-FTolP})_3]$,[31] infers that there is no electronic incentive for more than two formamidinate ligands to orientate about the di-potassium core. Instead, akin to the sodium analogue of **1** (see above), saturation of the metal centres in **1** and **2** is accomplished by THF donation.

In-view of the different molecular structures of THF and DME adducted FTolP complexes of lithium and sodium, *viz.*$[(\mu\text{-THF})\{Li(\mu\text{-}\eta^1\text{:}\eta^1\text{-FTolP})(THF)\}_2]\cdot 2THF \rightarrow [Li(DME)_3][Li_2(\mu\text{-}\eta^1\text{:}\eta^1\text{-FTolP})_3]$, $[Na_3(\mu_3\text{-}\eta^2\text{:}\eta^1\text{:}\eta^1\text{-FTolP})_2(\mu\text{-}\eta^2\text{:}\eta^2\text{-FTolP})(THF)_4] \rightarrow [\{Na(\mu\text{-}\eta^2\text{:}\eta^1\text{-FTolP})(\mu\text{-}\eta^1\text{:}\eta^1\text{-DME})\}_2]$,[31] the treatment of HFTolP with potassium hydride in DME was undertaken (Scheme 1). This afforded a solvent dependent colourless crystalline compound that characterised as [K(FTolP)(DME)] by $^1$H NMR, and presented NC(H)N resonances of 8.61 ppm and 163.6 ppm ($^1$H and $^{13}$C NMR resp. **2**; 8.92 ppm, 158.8 ppm) without apparent redistribution (no resonance equilibration over orthodox temperature range). The FTIR spectra of crystalline samples of [K(FTolP)(DME)] are devoid of the N–H stretch characteristic of HFTolP (strong absorption at *ca.* 3300 cm$^{-1}$). Accordingly, an X-ray structure determination was undertaken. From the outset, the significantly higher melting point of [K(FTolP)(DME)] relative to **1** and **2** (230 °C; 114 °C **1**, 152 °C **2**) inferred that the DME species exhibited a different molecular structure to the THF analogue. However, as the DME contained in [K(FTolP)-(DME)] correlated to the amount of THF in **1** under the proposed steric coordination numbers presented by Marçalo and Pires de Matos[47] (whereby coordinated DME accounts for *ca.* 1.5 coordinated THF ligands irrespective of coordination mode) a structural motif similar to those of **1** and **2** was also conceived.

The extended molecular structure of $[\{K(\mu\text{-}\eta^2\text{:}\eta^2\text{-FTolP})(\mu\text{-}\eta^2\text{:}\eta^1\text{-DME})\}_\infty]$, **3**, is depicted in Fig. 3 (POV-RAY[55] diagram, 30% thermal ellipsoids), selected bond-lengths and angles are listed in Table 1. Like the THF coordinated analogue **1**, compound **3** crystallises in the triclinic space group $P\bar{1}$ with half a dinuclear $\{K_2(\mu\text{-}\eta^2\text{:}\eta^2\text{-FTolP})_2(\mu\text{-}\eta^2\text{:}\eta^1\text{-DME})_2\}$ fragment in the asymmetric unit. Thus, unlike lighter Group 1 metal complexes of FTolP that include coordinated THF/DME ligands[31] the solid-state nature of **3** is not radically different from its THF congener. Prominent differences include diminished intra- and increased inter-$K_2$(formamidinate)$_2$ unit potassium–potassium distances of 3.4299(13) Å and 4.4760(14) Å, *cf.* mean intra- and inter-$K_2$(formamidinate)$_2$ potassium–potassium distances of **1** and **2** combined; 3.474 Å and 3.924 Å, and less disparate K–N contact distances due to increased formamidinate–potassium contact (mean 2.91 Å, longest K–N **1**; 3.148(2) Å, see Table 1). These differences are accentuated by the increased steric bulk of the bridging bis-DME unit of **3**, which possesses a well defined μ-η$^2$:η$^1$-binding mode, relative to the observably constrained $C_4H_8$ backbone tethers of the tris-THF bridging units of **1** or **2**. Akin to both THF species, the formation of a di-potassium di-formamidinate motif leads to putative potassium–carbon contacts, see Table 2, which are suggestive of η$^3$-diazaallyl bonding. However, contrary to **1** and **2**, the NCN backbones within the dinuclear moiety of **3** are

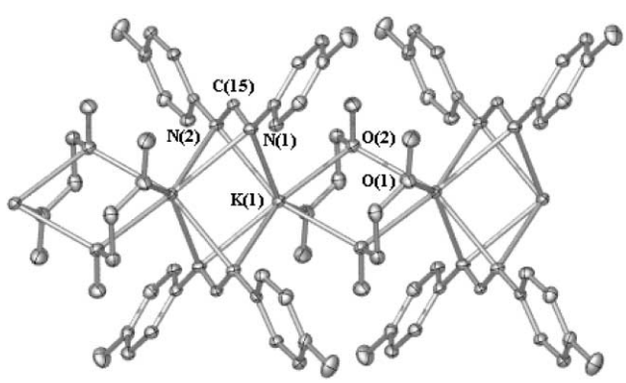


**Fig. 3** Molecular structure of $[\{K(\mu\text{-}\eta^2\text{:}\eta^2\text{-FTolP})(DME)\}_\infty]$, **3**. Four subunits of polymeric structure displayed, hydrogen atoms omitted for clarity.

placed more centrally (NKN plane to NCN plane angles 34.86(25)° and 45.29(27)°, see Table 2). In-spite of this, the greater metal–formamidinate proximity of **3** averts any lengthening of the K ··· C distances, which possess a mean of 3.19 Å (**1** and **2** also 3.19 Å). With respect to **1**, the effect of DME donors upon the $K_2$(formamidinate)$_2$ core does not impact as highly as the *meta*-methyl tolyl groups of **2**. These render the backbone NCN angles of **2** smaller (mean 120.3°, **1**; 121.4°, **3**; 121.4(2)°). The *para*-tolyl groups of **3** exist at a mean dihedral angle of 28.08° to the NCN backbone plane, whilst in contrast to both **1** and **2**, wherein the $K_2$(formamidinate)$_2$ units exist at significant relative torsion angles (see Table 1); the $K_2$(formamidinate)$_2$ units of **3** are necessarily aligned as a prerequisite of crystallographic symmetry. Superficially, this is the major difference between **3** and the related structures of **1** and **2**.

The intra-dinuclear unit bond-lengths and angles of complexes **1**–**3** bear a close resemblance to those of **6**–**8**, the mean K–N lengths and NKN, NCN backbone angles being 2.92 Å, 46.6°, 121.4° (**1**), 2.909 Å, 46.3°, 120.3° (**2**) and 2.91 Å, 46.2°, 121.4(2)° (**3**) (mean of **6**–**8** 2.793 Å, 46.9°, 117.5°).[36–38] These do not differ greatly from those within related monoanionic β-dinitrogen ligand complexes, such as [$K_2${μ-η$^2$:η$^2$-2-($C_5H_4N$)-NPh}$_2$(tmeda)$_2$],[39] in which the analogous lengths and angles have a mean of 2.83 Å, 47.42° and 113.86°. Overall, the mean K–N lengths within **1**–**3** compare favourably to the mean structurally characterised K–N bond (2.939 Å),[43] whilst the intra-ligand C–N backbone lengths deviate by no more than 0.005 Å (**1**), 0.004 Å (**2**) and 0.005 Å (**3**) within each complex, thereby denoting electron delocalisation of the formamidinate ligands therein (HFTolP discrete single and double C–N bonds of 1.346(6) Å and 1.281(6) Å).[30] Meanwhile, the μ-η$^2$:η$^1$-DME binding motif of **3** has precedent in the DME adduct of potassium cyclopentadienide[42] and a DME solvated caesium dicarborane cobalt salt.[48] The former displays a mean K–O distance of 2.85 Å and mean OKO chelate angle of 58.71° (**3**; 2.81 Å, 60.46(6)° resp.).[42] Unfortunately, the high aerobic and moisture sensitivity of compounds **1**–**3** (and **4**, see below), combined with their facile loss of solvent (as reported for [{Li(μ-η$^2$:η$^1$-FTolP)($Et_2O$)}$_2$]),[30] frustrated the acquisition of meaningful mass spectrometric and C, H, N microanalytical data. However, given that $^1$H NMR spectra of **1**–**3** (and **4**, see below) show no observable impurities, and in-view of the sharpness of their melting points, we believe the bulk purity of **1**–**3** (and **4**) to be of microanalytical quality.

The apparent necessity of supplementary donors in **1**–**3** and absence of donors in **5**, which leads to an unprecedented formamidinate binding mode,[35] invites investigation as to the likely solid-state nature of a solvent free analogue. To address this a toluene solution of HFTolP was treated with a slurry of potassium hydride under similar conditions to the preparation of **1**–**3** (Scheme 1), resulting in precipitation of a colourless microcrystalline product that could not be characterised by spectroscopy due to low solubility in non-donating solvents. The structural nature of this compound, which we believe to be polymeric, is still under investigation, however, addition of excess 18-crown-6 (>3.0 equivalents, 18-crown-6 being the size-fit complement of potassium) initiated immediate dissolution of the insoluble material providing a deep orange solution (Scheme 1). Removal of all reaction volatiles *in vacuo* followed by washing with cold hexane gave a colourless material that characterised as [K(FTolP)(18-crown-6)], **4**, by $^1$H NMR ($C_6D_6$). As for **1**–**3**, the absence of protonated ligand attributable N–H resonances and stretches indicated deprotonation, as did the new positioning of the NC(H)N resonances at 9.15 ppm and 185.5 ppm ($^1$H and $^{13}$C NMR resp.), those of the ligand appearing at lower frequency (8.01 ppm, 150.4 ppm).[31] Large prismatic crystals of **4** were grown from toluene and an X-ray structure determination undertaken (see Fig. 4, POV-RAY[55] diagram, 30% thermal ellipsoids). Unlike **1**–**3**, compound **4** is not sensitive to solvent loss, however, its sensitivity to air and moisture is equally pronounced decomposing rapidly to an orange oil upon brief (within seconds) exposure to air. Relevant bond-lengths and angles are listed in Table 1.

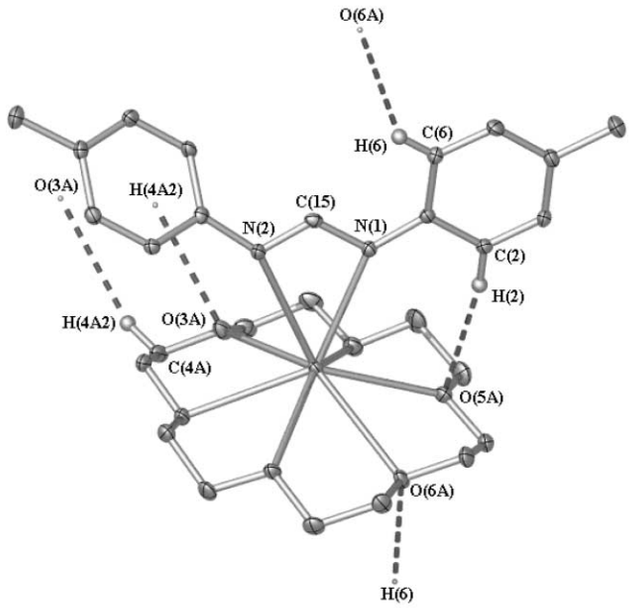


**Fig. 4** Molecular structure of [K(η$^2$-FTolP)(18-crown-6)], **4**. Hydrogens of H-bond donors displayed, all other hydrogen atoms omitted for clarity. C–H ··· O Hydrogen bond lengths (Å) and angles (°): O(3A)$^a$ ··· H(4A2)$^b$ 2.8621, O(3A)$^a$ ··· C(4A)$^b$ 3.7542(42), O(5A) ··· H(2) 2.5496, O(5A) ··· C(2) 3.4753(41), O(6A)$^c$ ··· H(6)$^d$ 2.546, O(6A)$^c$ ··· C(6)$^d$ 3.3758(41); O(3A) ··· H(4A2)–C(4A)$^{a,b}$ 150.30, O(5A) ··· H(2)–C(2) 164.79, O(6A) ··· H(6)–C(6)$^{c,d}$ 143.49. Symmetry transformations used to generate equivalent atoms: $^a$1 − *x*, −*y*, 1 − *z*. $^b$1 − *x*, −*y*, 1 − *z*. $^c$½ + *x*, ½ − *y*, *z* − ½. $^d$*x* − ½, ½ − *y*, ½ + *z*.

In the solid-state, complex **4** represents the first poly-ether crown adducted monomeric Group 1 amidinate. The FTolP ligand coordinates in an η$^2$-chelate fashion juxtaposed to an η$^6$-bound crown (crown-$O_6$-centroid–K(1)–C(15) angle 170.88(58)°). The potassium resides in a distorted eight-coordinate environment (O(1A)–K(1)–O(2A) 58.26(5)°, O(1A)–K(1)–N(1) 122.52(6)°) with unsymmetrical K–N bonds of 2.829(2) Å and 2.923(2) Å, and a mean K–O bond length of 2.93 Å (**3**; 2.81 Å). The discrepancy in K–N bonds is not alluded to by the intra-FTolP C–N bonds of 1.323(3) Å and 1.323(3) Å, which indicate complete charge delocalisation across the NCN unit (HFTolP C–N bonds of 1.346(6) Å and 1.281(6) Å, variation 0.065 Å; localised single and double C–N bonds).[30] However, the tolyl groups of **4** exist at an inordinately large torsion angle to one-another (47.98(14)°) and contrasting dihedral angles to the formamidinate NCN backbone (14.24(58)°, 33.94(41)°). This appears to result from the intra-molecular interaction of O(5A) (see Fig. 4) with a proton upon the C(1)–C(6) tolyl ring (H(2)), and inter-molecular interactions of O(6A) with H(6) upon the same tolyl ring of an adjacent unit and O(3A) with H(4A2) on a neighbouring unit of **4** within the crystal lattice (see Figs. 4 and 5). This intra-molecular interaction may be the origin of the disparity in K–N bond-lengths, the shorter length being proximal to the O(5A) ··· H(2) contact. All three hydrogen-bonding interactions are within the accepted contact for oxygen ··· hydrogen–carbon H-bonds (C ··· O 3.0–4.0 Å,[49] O(5A) ··· C(2) 3.4753(41) Å, O(5A) ··· H(2) 2.5496 Å, O(6A) ··· C(6) 3.3758(41) Å, O(6A) ··· H(6) 2.5646 Å, O(3A) ··· C(4A) 3.7542(42) Å, O(3A) ··· H(4A2) 2.8621 Å) and, hence, like the H-bonded structural motif of **5**, provide **4** with a polymeric supramolecular structure. As displayed in Fig. 5, the resulting network can be described as polymeric one-dimensional chains of **4** intermittently linked, in a

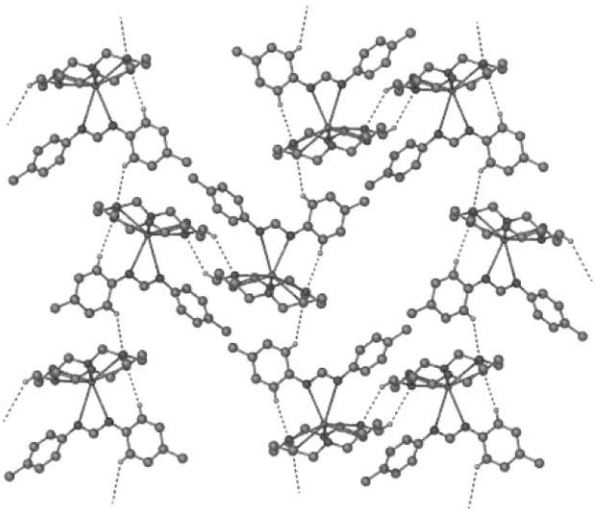

**Fig. 5** Supramolecular structure of [K(η²-FTolP)(18-crown-6)], **4**, illustrating two-dimensional H-bonded network.

'pseudo-isotactic' manner, perpendicular to the direction of chain propagation by O(3A) ··· H(4A2) contacts (two per unit) to two adjoining strands that run in the opposing direction. This creates a 'checker-board' like supramolecular motif. These interactions appear to be a solid-state phenomenon since no discernable lack of symmetry is observed in solution state NMR spectra. Finally, the η²-formamidinate potassium chelation of **4**, which occurs without supplementary coordination of bridging ligands, renders the backbone NCN and NKN angles of **4** obtuse relative to those of **1**–**3**; 122.7(3)°, 47.59(6)° respectively (**1**; mean 121.4°, 46.6°). This is unsurprising given the mono- and not bi-nuclear chelate binding mode of the *N*,*N*′-di(tolyl)formamidinate ligand.

## Experimental

The formamidinate ligand precursors *N*,*N*′-di(*para*-tolyl)- and *N*,*N*′-di(*meta*-tolyl)formamidine ((Tol)NC(H)N(H)(Tol)), HFTolP and HFTolM respectively, were synthesised according to a published procedure.[30,50] Potassium hydride under mineral oil was purchased from Aldrich and isolated by decantation followed by washing with dried and degassed hexane. Tetrahydrofuran (THF), 1,2-dimethoxyethane (DME), toluene and hexane were dried over sodium, freshly distilled from sodium–potassium alloy, and freeze–thaw degassed prior to use. All manipulations were performed using conventional Schlenk or glovebox techniques under an atmosphere of high purity dinitrogen in flame-dried glassware. Infrared spectra were recorded as Nujol mulls using sodium chloride plates on a Nicolet Nexus FTIR spectrophotometer. $^1$H NMR spectra were recorded at 300.13 MHz and $^{13}$C NMR spectra were recorded at 75.46 MHz using a Bruker DPX 300 spectrometer, and chemical shifts were referenced to the residual $^1$H or $^{13}$C resonances of the deutero-benzene solvent. Melting points were determined in sealed glass capillaries under dinitrogen and are uncorrected. The high aerobic and moisture sensitivity of compounds **1**–**4**, combined with the facile loss of solvent from **1**–**3** (as reported for [{Li(μ-η²:η¹-FTolP)(Et$_2$O)}$_2$]),[30] frustrated the acquisition of meaningful mass spectrometric and C, H, N microanalytical data. However, given that $^1$H NMR spectra of **1**–**4** show no observable impurities, and in-view of the sharpness of their melting points, we believe the bulk purity of **1**–**4** to be of microanalytical quality.

### [{K$_2$(μ-η²:η²-FTolP)$_2$(μ-THF)$_3$}$_\infty$] (1)

Potassium hydride (0.10 g, 2.50 mmol) was added as a stirred slurry (THF, 25 cm$^3$) to a solution of HFTolP (0.50 g, 2.23 mmol) in THF (20 cm$^3$). This resulted in the formation of an opaque green solution that was stirred for *ca.* 6 h prior to moderate heating, which produced a clear deep orange solution. Placement at −10 °C after filtration and concentration *in vacuo* yielded the title compound as colourless needles (0.36 g, 44%), mp 114 °C. $^1$H NMR (C$_6$D$_6$, 300 K): *δ* 1.42 (m, 12H, C*H*$_2$, THF), 2.19 (s, 12H, Ar–C*H*$_3$), 3.56 (m, 12H, C*H*$_2$O, THF), 6.93 (d, 8H, Ar-*H*), 7.02 (d, 8H, Ar-*H*), 8.15 (s, 2H, NC(*H*)N). $^{13}$C NMR (C$_6$D$_6$, 300 K): *δ* 21.2 (s, Ar-*C*H$_3$), 26.2 (s, *C*H$_2$, THF), 68.2 (s, *C*H$_2$O, THF), 119.9, 129.3, 130.5, 132.0 (s, Ar-*C*), 162.3 (s, N*C*(H)N). IR (Nujol) *ν*/cm$^{-1}$: 808m, 819m, 872m, 1022w, 1120w, 1315m, 1505m, 1670s.

### [({K$_2$(μ-η²:η²-FTolM)$_2$(μ-THF)$_3$}·THF)$_\infty$] (2)

Potassium hydride (0.10 g, 2.50 mmol) was added as a stirred slurry (THF, 25 cm$^3$) to a solution of HFTolM (0.39 g, 1.74 mmol) in THF (15 cm$^3$). After initial effervescence, the solution was heated moderately (*ca.* 60 °C) for 3 hours rendering a light colourless precipitate. Filtration, concentration *in vacuo* and placement at −15 °C yielded the title compound as air-sensitive, solvent dependent large yellow prisms (0.65 g, 78%), mp 152 °C. $^1$H NMR (C$_6$D$_6$, 300 K): *δ* 1.44 (m, 12H, C*H*$_2$, THF), 2.29 (s, 12H, Ar-C*H*$_3$), 3.53 (m, 12H, C*H*$_2$O, THF), 6.75 (m, 4H, Ar-*H*), 6.88 (m, 8H, Ar-*H*), 7.17 (m, 4H, Ar-*H*), 8.92 (s, 2H, NC(*H*)N). $^{13}$C NMR (C$_6$D$_6$, 300 K): *δ* 20.4 (s, Ar-*C*H$_3$), 24.4 (s, *C*H$_2$, THF), 66.5 (s, *C*H$_2$O, THF), 116.0, 119.8, 127.1, 128.1, 137.4, 143.0 (s, Ar-*C*), 158.8 (s, N*C*(H)N). IR (Nujol) *ν*/cm$^{-1}$: 697m, 764w, 784w, 878w, 919w, 984w, 1043m, 1074m, 1148m, 1239w, 1257m, 1318s, 1467s, 1525s, 1596w sh, 1651w.

### [{K(μ-η²:η²-FTolP)(μ-η²:η¹-DME)}$_\infty$] (3)

Potassium hydride (0.20 g, 2.24 mmol) was added as a stirred slurry (DME, 20 cm$^3$) to a solution of HFTolP (0.50 g, 2.23 mmol) in DME (20 cm$^3$). This resulted in the formation of a colourless opaque solution that progressively turned green. Once no further colour change was observed the solution was filtered, concentrated *in vacuo* and placed at −10 °C. Over a period of several weeks, this yielded the title compound as small colourless crystals (0.47 g, 60%), mp 230 °C. $^1$H NMR (C$_6$D$_6$, 300 K): *δ* 2.48 (s, 6H, Ar-C*H*$_3$), 3.14 (s, 6H, OC*H*$_3$, DME), 3.33 (s, 4H, OC*H*$_2$, DME), 6.88 (d, 4H, Ar-*H*), 7.01 (d, 4H, Ar-*H*), 8.61 (s, 1H, NC(*H*)N). $^{13}$C NMR (C$_6$D$_6$, 300 K): *δ* 21.4 (s, Ar-*C*H$_3$), 62.1 (s, O*C*H$_3$, DME), 70.9 (s, O*C*H$_2$, DME), 120.5, 127.3, 130.6, 131.5 (s, Ar-*C*), 163.6 (s, N*C*(H)N). IR (Nujol) *ν*/cm$^{-1}$: 762w, 823m, 865m, 1020w, 1116w, 1308m, 1505m, 1665s.

### [K(η¹:η¹-FTolP)(18-crown-6)] (4)

Potassium hydride (0.20 g, 4.99 mmol) was added as a stirred slurry (toluene, 30 cm$^3$) to a solution of HFTolP (0.50 g, 2.23 mmol) and 18-crown-6 (0.60 g, 2.27 mmol) in toluene (40 cm$^3$). This resulted in an opaque orange solution that was stirred overnight and allowed to settle. Placement at −10 °C over a period of several days, after filtration and concentration *in vacuo*, yielded the title compound as small colourless prisms (0.73 g, 62%), mp 168 °C. $^1$H NMR (C$_6$D$_6$, 300 K): *δ* 2.35 (s, 6H, Ar-C*H*$_3$), 3.20 (s, 24H, OC*H*$_2$), 6.93 (d, 4H, Ar-*H*), 7.03 (d, 4H, Ar-*H*), 9.15 (s, 1H, NC(*H*)N), $^{13}$C NMR (C$_6$D$_6$, 300 K): *δ* 21.6 (s, Ar-*C*H$_3$), 70.5 (s, O*C*H$_2$), 121.3, 126.0, 129.7, 130.0 (s, Ar-*C*), 185.5 (s, N*C*(H)N). IR (Nujol) *ν*/cm$^{-1}$: 818m, 860w, 932w, 1032w, 1128w, 1299m, 1509m, 1670s.

### X-Ray crystallography

Crystalline samples of compounds **1**–**4** were mounted upon glass fibres, in viscous hydrocarbon oil at −150 °C (123 K). Crystal data were obtained using an Enraf-Nonius Kappa CCD. X-Ray data were processed using the DENZO

**Table 3** Summary of crystal data for compounds **1**–**4**

| | [{$K_2$(μ-η²:η²-FTolP)$_2$-(μ-THF)$_3$}$_\infty$] (**1**) | [({$K_2$(μ-η²:η²-FTolM)$_2$-(μ-THF)$_3$}·THF)$_\infty$] (**2**) | [{K(μ-η²:η²-FTolP)-(μ-η²:η¹-DME)}$_\infty$] (**3**) | [K(η²-FTolP)$_2$-(18-crown-6)] (**4**) |
|---|---|---|---|---|
| Mol. formula | $C_{42}H_{54}N_4O_3K_2$ | $C_{46}H_{62}N_4O_4K_2$ | $C_{19}H_{25}N_2O_2K$ | $C_{27}H_{39}N_2O_6K$ |
| Mol. weight | 741.09 | 813.20 | 352.49 | 526.70 |
| Temperature/K | 123(2) | 123(2) | 123(2) | 123(2) |
| Crystal system | Triclinic | Triclinic | Triclinic | Monoclinic |
| Space group | $P\bar{1}$ | $P\bar{1}$ | $P\bar{1}$ | $P2_1/n$ |
| *a*/Å | 11.613(2) | 13.325(5) | 7.7331(11) | 9.3213(19) |
| *b*/Å | 14.042(3) | 13.843(5) | 10.4662(14) | 23.917(5) |
| *c*/Å | 14.724(3) | 14.742(5) | 13.3689(19) | 13.559(3) |
| *α*/° | 114.64(3) | 66.345(5) | 107.764(3) | 90 |
| *β*/° | 105.23(3) | 73.400(5) | 90.529(3) | 109.56(3) |
| *γ*/° | 99.57(3) | 63.731(5) | 108.107(3) | 90 |
| Volume/Å$^3$ | 1998.9(7) | 2214.1(14) | 972.9(2) | 2848.4(10) |
| *Z* | 2 | 2 | 2 | 4 |
| $D_c$/g cm$^{-3}$ | 1.231 | 1.220 | 1.203 | 1.228 |
| $\mu$/mm$^{-1}$ | 0.279 | 0.260 | 0.285 | 0.227 |
| Reflections collected | 33627 | 40214 | 6518 | 14959 |
| Unique reflections | 9721 | 10799 | 4496 | 6990 |
| Parameters varied | 464 | 509 | 317 | 327 |
| *R*(int) | 0.0652 | 0.0667 | 0.0546 | 0.0952 |
| $R_1$ | 0.0650 | 0.0491 | 0.0632 | 0.0499 |
| $wR_2$ | 0.1489 | 0.1289 | 0.1457 | 0.0745 |

program.[51] Structural solution and refinement was carried out using the SHELX suite of programs[52,53] with the graphical interface X-Seed.[54] All hydrogen atoms were placed in calculated positions using the riding model. Crystal data and refinement parameters for all complexes are compiled in Table 3.

CCDC reference numbers 188555 (for **1**), 191452 (for **2**), 188557 (for **3**) and 188558 (for **4**).

See http://www.rsc.org/suppdata/dt/b2/b206165a/ for crystallographic data in CIF or other electronic format.

## Conclusion

The metallation of *N*,*N*′-di(tolyl)formamidines with potassium in the presence of a strong monodentate or chelating bidentate ethereal donor, *i.e.* THF or DME, affords potassium formamidinate molecular structures that, unlike other solvated Group 1 benzamidinate/guanidinate complexes,[36–38] do not possess low aggregation but do exhibit di-potassium di-μ-η²:η²-amidinate units. With regard to archival structural data,[43,44] it can be argued that these units approach μ-η³:η² or μ-η³:η³ formamidinate binding. The formamidinate coordination modes μ-η²:η², μ-η³:η² and μ-η³:η³ are unprecedented in formamidinate chemistry.[43,45,46]

The presence of *meta*-methyl groups in **2** imposes extended potassium–nitrogen contacts and concomitantly smaller NCN backbone angles resulting from increased tolyl-methyl steric buttressing with adjacent formamidinates, ancillary THF donors and the NC(H)N backbone proton. Replacement of coordinated THF by DME does not result in a different dinuclear solid-state motif. This is contrary to both lithium and sodium findings, where the replacement of THF by DME leads to salt formation or decreased aggregation respectively.[31] This homologous structural preference controverts the proposal that extended structural diversity may result from minor modification of the potassium formamidinate reaction medium, as suggested in the introduction, and is hence unfounded. This is presumably because the larger ionic radius of potassium[14] enables greater conformational dexterity of the ligand, thereby increasing the likelihood of similar ligand binding modes prior to the inclusion of ancillary donors. The use of a macrocyclic poly-ether donor, *i.e.* 18-crown-6, disrupts the infinite aggregation and μ-η²:η²-coordination of **1**–**3**, leading to monomeric complex **4**. Complex **4** exhibits both intra- and inter-molecular C–H ··· O hydrogen bonding. This leads to a two-dimensional supramolecular structure in the solid-state.


## Acknowledgements

The authors would like to acknowledge the Australian Research Council for their continued support. J. B. and C. B. thank the Deutsche Studienstiftung and Friedrich Ebert Stiftung (resp.) for financial support. M. L. C. would like to thank the Royal Society for the provision of a postdoctoral fellowship.


## References and notes


1 M. F. Lappert, P. P. Power, A. R. Sanger and R. C. Srivastava, *Metal and Metalloid Amides*, Ellis Horwood Ltd., Chichester, 1980.
2 W. N. Setzer and P. v. R. Schleyer, *Adv. Organomet. Chem.*, 1985, **24**, 353.
3 K. Gregory, P. v. R. Schleyer and R. Snaith, *Adv. Inorg. Chem.*, 1991, **37**, 47.
4 R. E. Mulvey, *Chem. Soc. Rev.*, 1991, **20**, 176.
5 D. S. Wright and M. A. Beswick, ch. 1 in *Comprehensive Organometallic Chemistry*, 2nd edn., vol. 1, p. 1, eds. E. W. Abel, F. G. A. Stone and G. Wilkinson, Pergamon, Oxford, 1995.
6 D. Seebach, *Angew. Chem., Int. Ed. Engl.*, 1988, **27**, 1624.
7 D. R. Armstrong, D. Barr, W. Clegg, R. E. Mulvey, D. Reed, R. Snaith and K. Wade, *J. Chem. Soc., Chem. Commun.*, 1986, 869.
8 T. Fjeldberg, P. B. Hitchcock, M. F. Lappert and A. J. Thorne, *J. Chem. Soc., Chem. Commun.*, 1984, 822.
9 M. Majewski and D. M. Gleave, *J. Organomet. Chem.*, 1994, **470**, 1.
10 B. J. Wakefield, *Organolithium Methods*, Academic Press, New York, 1988.
11 *Lithium Chemistry: A Theoretical and Experimental Overview*, eds. A. M. Sapsa and P. v. R. Schleyer, Wiley-Interscience, New York, 1995.
12 M. Gray, M. Tinkl and V. Snieckus, in *Comprehensive Organometallic Chemistry*, 2nd edn., eds. E. W. Abel, F. G. A. Stone and G. Wilkinson, Pergamon, Oxford, 1995, vol. 11, p. 1.
13 C.H. Heathcock, in *Comprehensive Carbanion Chemistry*, eds. E. Buncel, T. Durst, Elsevier, New Yourk, 1980, B, Ch. 4.
14 E. Fluck and K. G. Heumann, *Periodic Table of the Elements*, VCH, Weinheim, Germany, 1991.
15 F. A. Cotton, L. M. Daniels and C. A. Murillo, *Inorg. Chem.*, 1993, **32**, 2881.
16 F. A. Cotton, L. M. Daniels, L. R. Falvello and C. A. Murillo, *Inorg. Chim. Acta*, 1994, **219**, 7.
17 F. A. Cotton, L. M. Daniels, D. J. Maloney and C. A. Murillo, *Inorg. Chim. Acta*, 1996, **249**, 9.
18 F. A. Cotton, L. M. Daniels, L. R. Falvello, J. H. Matonic, C. A. Murillo, X. Wang and H. Zhou, *Inorg. Chim. Acta*, 1997, **266**, 91.
19 F. A. Cotton, L. M. Daniels and C. A. Murillo, *Angew. Chem., Int. Ed. Engl.*, 1992, **31**, 737.
20 J. A. R. Schmidt and J. Arnold, *Chem. Commun.*, 1999, 2149.

21 K. Kincaid, C. P. Gerlach, G. R. Giesbrecht, J. R. Hagadorn, G. D. Whitener, A. Shafir and J. Arnold, *Organometallics*, 1999, **18**, 5360.
22 G. D. Whitener, J. Hagadorn and J. Arnold, *J. Chem. Soc., Dalton Trans.*, 1999, 1249.
23 D. Abeysekera, K. N. Robertson, T. S. Cameron and J. A. C. Clyburne, *Organometallics*, 2001, **20**, 5532.
24 Y. Zhou and D. S. Richeson, *Inorg. Chem.*, 1996, **35**, 2448.
25 Y. Zhou and D. S. Richeson, *Inorg. Chem.*, 1997, **36**, 501.
26 S. R. Foley, Y. Zhou, G. P. A. Yap and D. S. Richeson, *Inorg. Chem.*, 2000, **39**, 924.
27 S. Dagorne, R. F. Jordan and V. G. Young Jr, *Organometallics*, 1999, **18**, 4619.
28 M. P. Coles, D. C. Swenson, R. F. Jordan and V. G. Young Jr, *Organometallics*, 1997, **16**, 5183.
29 S. Dagorne, I. A. Guzei, M. P. Coles and R. F. Jordan, *J. Am. Chem. Soc.*, 2000, **122**, 274.
30 F. A. Cotton, S. C. Haefner, J. H. Matonic, X. Wang and C. A. Murillo, *Polyhedron*, 1997, **16**, 541.
31 M. L. Cole, P. C. Junk and L. M. Louis, *J. Chem. Soc., Dalton Trans.*, 2002, 3906.
32 M. L. Cole, D. J. Evans, L. M. Louis and P. C. Junk, *New J. Chem.*, 2002, **26**, 1015.
33 K. H. den Haan, J. L. de Boer, J. H. Teuben, A. L. Spek, B. Kojic-Prodic, G. R. Hays and R. Huis, *Organometallics*, 1986, 1726.
34 W. J. Evans, J. W. Grate, K. R. Levan, I. Bloom, T. T. Peterson, R. J. Doedens, H. Zhang and J. L. Atwood, *Inorg. Chem.*, 1986, **25**, 3614.
35 J. Baldamus, C. Berghof, M. L. Cole, D. J. Evans, E. Hey-Hawkins and P. C. Junk, *J. Chem. Soc., Dalton Trans.*, 2002, 2802.
36 G. R. Giesbrecht, A. Shafir and J. Arnold, *J. Chem. Soc., Dalton Trans.*, 1999, 3601.
37 P. B. Hitchcock, M. F. Lappert and D.-S. Liu, *J. Organomet. Chem.*, 1995, **488**, 241.
38 P. B. Hitchcock, M. F. Lappert and M. Layh, *J. Chem. Soc., Dalton Trans.*, 1998, 3113.
39 P. C. Andrews, D. R. Baker, R. E. Mulvey, W. Clegg and P. O. O'Neill, *Polyhedron*, 1991, **10**, 1839.
40 S. T. Liddle and W. Clegg, *J. Chem. Soc., Dalton Trans*, 2001, 402.
41 The Cambridge Crystallographic Structural Database (CCSD) contains 39 examples of bridging tetrahydrofuran of which two contain double bridging THF units. None display the triple bridging THF motif of the complexes described herein.
42 M. L Cole, C. Jones and P. C. Junk, *J. Chem. Soc., Dalton Trans.*, 2002, 896.
43 From a survey of the CCSD.
44 F. Feil and S. Harder, *Organometallics*, 2000, **19**, 5010.
45 The $\mu$-$\eta^3$:$\eta^2$-amidinate coordination mode has been observed twice in *N*,*N*′-di(isopropyl)acetamidinate complexes of ruthenium pentamethylcyclopentadiene; H. Kondo, Y. Yamaguchi and N. Nagashima, *J. Am. Chem. Soc.*, 2001, **123**, 500.
46 The $\eta^3$-amidinate coordination mode has been observed in ref. 45 and *N*,*N*′-di(*tert*-butyl)-/*N*,*N*′-di(cyclohexyl)benzamidinate complexes of ruthenium pentamethylcyclopentadiene; Y. Yamaguchi and N. Nagashima, *Organometallics*, 2000, **19**, 725.
47 From the steric coordination number defined for lanthanoid and actinoid complexes defined in; J. Marçalo and A. Pires de Matos, *Polyhedron*, 1989, **8**, 2431 . Relevant as, like *f*-block elements, the coordination of Group 1 metals is largely non-directional (isotropic) contrary to d-block chemistry where metallic geometry is rigid due to electronic constraints.
48 R. M. Chamberlin, B. L. Scott, M. M. Meli and K. D. Abney, *Inorg. Chem.*, 1997, **36**, 809.
49 J. W. Steed and J. L. Atwood, *Supramolecular Chemistry*, 2000, Wiley, Chichester, England.
50 R. M. Roberts, *J. Org. Chem.*, 1949, **14**, 277.
51 Z. Otwinowski and W. Minor, *"Processing of X-ray Diffraction Data Collected in Oscillation Mode", Methods in Enzymology, 276: Macromolecular Crystallography, Part A*, eds. C. W. Cater and R. M. Sweet, Academic Press, New York, 1997, vol. 307.
52 G. M. Sheldrick, SHELXL-97, University of Göttingen, Germany, 1997.
53 G. M. Sheldrick, SHELXS-97, University of Göttingen, Germany, 1997.
54 L. J. Barbour, X-Seed, Crystallographic Interface, University of Missouri-Columbia, MO, USA, 1999.
55 POV-RAY, Ray Tracing Program, www.povray.org.